ChemElectroChem

Chemistry Europe
European Chemical Societies Publishing
ChemElectroChem

RESEARCH ARTICLE OPEN ACCESS

A Cathodic Hydrogen Atom Transfer Strategy for Electrochemical Carboxylation of Dibenzylic C(sp^3)—H Bonds With CO_2

Yuto Maeji[1] | Toshimichi Kobayashi[1] | Kento Kosugi[2] | Yutaka Saga[1,3] | Masanari Hirahara[4] | Mio Kondo[2] | Tetsuya Kambe[1,3] | Shigeyuki Masaoka[1,3]

[1]Division of Applied Chemistry, Graduate School of Engineering, The University of Osaka, Suita, Osaka, Japan | [2]Department of Chemistry, School of Science, Institute of Science Tokyo, Meguro-ku, Tokyo, Japan | [3]Innovative Catalysis Science Division, Institute for Open and Transdisciplinary Research Initiatives (ICS-OTRI), The University of Osaka, Suita, Osaka, Japan | [4]Department of Applied Chemistry, Faculty of Engineering, Osaka Institute of Technology, Asahi Ward, Osaka, Japan

Correspondence: Yutaka Saga (ysaga@chem.eng.osaka-u.ac.jp) | Shigeyuki Masaoka (masaoka@chem.eng.osaka-u.ac.jp)

Received: 14 February 2026 | **Revised:** 13 March 2026 | **Accepted:** 1 April 2026

Keywords: C(sp^3)—H bonds | carbon dioxide utilization | electrosynthesis | hydrogen atom transfer

ABSTRACT

Direct carboxylation of C(sp^3)—H bonds with carbon dioxide (CO_2) offers an attractive route to value-added carboxylic acids but remains challenging due to the inertness of both reaction partners. Here, we report a fundamentally distinct electrochemical strategy that enables carboxylation of dibenzylic C(sp^3)—H bonds using hydrogen atom transfer (HAT) species reductively generated at the cathode. This represents a rare example of C(sp^3)—H bond functionalization mediated by cathodically generated HAT species. In contrast to anodic HAT systems that require interelectrode diffusion of reactive intermediates, the present method allows all the elementary steps (HAT species generation, C(sp^3)—H bond cleavage, and CO_2 incorporation) to occur at the same cathode. Consequently, the reaction proceeds efficiently under mild conditions (room temperature, 1 atm CO_2) without requiring an external sacrificial redox reagent, affording carboxylation products in good yields (up to 69%) within a short reaction time (2 h). Mechanistic studies support a pathway involving sequential electron transfer-chemical reaction (EC) and CO_2-coupled electron transfer processes for HAT species generation. This work establishes a mechanistically defined platform for electrochemical dibenzylic C(sp^3)—H bond functionalization.

1 | Introduction

Upgrading carbon dioxide (CO_2) into value-added chemicals has emerged as a key strategy toward a sustainable chemical economy [1–4]. In this context, carboxylation with CO_2 is a powerful and sustainable synthetic approach [5–11] because it directly affords carboxylic acids, important structural motifs found in pharmaceuticals, biologically active molecules, and fine chemicals [12]. Among such transformations, the direct carboxylation of C(sp^3)—H bonds [13], which are ubiquitous in organic molecules [14–18], represents an ideal approach to producing valuable chemicals from abundant resources. However, this transformation remains highly challenging due to the inherent inertness of both reaction partners: CO_2 possesses high thermodynamic stability and kinetic inertness, and C(sp^3)—H bonds typically exhibit strong bond dissociation energies. To overcome these challenges, various strategies have been developed, including metal reagents [19–21] and photoredox catalysis [22–29]. Despite the significant progress, most reported systems still require energy-demanding harsh conditions, such as high temperature, high pressure of CO_2, the use of excess amounts of redox reagents, or UV irradiation.

Electrochemical transformation offers a promising alternative (Figure 1a) [30–34]. In this approach, electron transfer at

Yuto Maeji and Toshimichi Kobayashi contributed equally to this study.

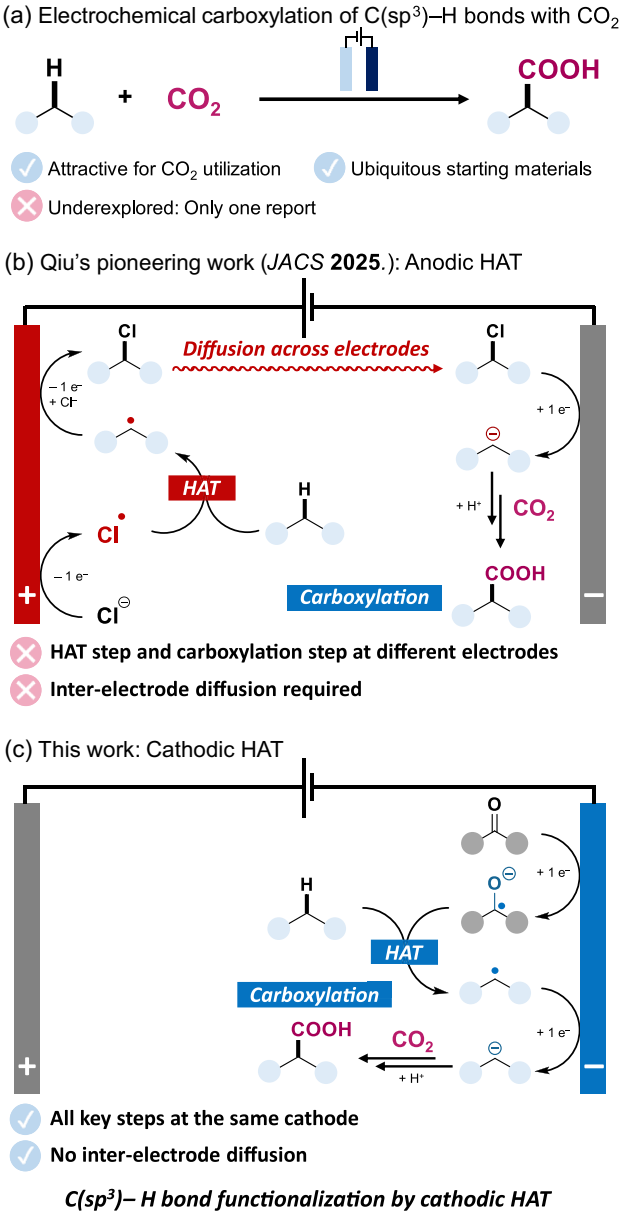

FIGURE 1 | (a) Electrochemical carboxylation of C(sp^3)—H bonds with CO_2. (b) Pioneering work by Qiu et al.: Anodic HAT. (c) This work: Cathodic HAT.

electrodes can be precisely controlled by the applied potential, thereby enabling reactions under mild conditions without the need for high temperature and sacrificial redox reagents. Very recently, Qiu et al. reported the first electrochemical carboxylation of benzylic C(sp^3)—H bonds with CO_2 (Figure 1b) [35]. In their system, chlorine radicals generated oxidatively from dichloroethane (DCE) at the anode mediates hydrogen atom transfer (HAT) [36–39] process to cleave benzylic C(sp^3)—H bonds. Despite this notable achievement, there is a critical limitation: the substrate radical intermediates are generated at the anode, whereas productive CO_2 incorporation fundamentally requires formation of the corresponding carbanion species at the cathode. Consequently, this system inherently relies on the diffusion of these intermediates across electrodes, which significantly restricts both its practicality and generality. A system that generates the HAT species reductively at the cathode and enables both C(sp^3)—H bond cleavage and subsequent CO_2 incorporation at the same electrode would overcome this fundamental limitation. However, cathodic generation of HAT species has remained underdeveloped, and there have been only limited reports on such reductively-generated HAT species at cathode for C(sp^3)—H bond functionalization, including a recent study employing redox-active carbonate system [40], although electrochemically driven HAT-mediated C(sp^3)—H functionalization in general has recently attracted increasing attention in organic electrosynthesis [41].

Here, we report, as a proof of concept, an electrochemical carboxylation of dibenzylic C(sp^3)—H bonds enabled by HAT species reductively generated at the cathode, using fluorene as a model substrate (Figure 1c). This represents a rare example of C(sp^3)—H bond functionalization mediated by cathodically generated HAT species. The reaction proceeds smoothly under mild conditions, such as at room temperature, under 1 atm CO_2, and without the use of any metals or external sacrificial redox reagents, although benzil functions as a stoichiometric reagent in the reaction. Notably, direct generation of the HAT species at the cathode allows the overall CO_2 incorporation process to occur at the same electrode, without requiring diffusion of intermediates between electrodes. Furthermore, mechanistic studies, including electrochemical measurements, cyclic voltammetry (CV) simulations, and controlled potential electrolysis (CPE) experiments, support that cathodic HAT generation is crucial for this transformation. Collectively, our strategy differs from previously reported HAT-enabled electrochemical systems and electrocarboxylation approaches in that the HAT species arises from a reduced intermediate under CO_2 conditions, and the key steps of C(sp^3)—H bond activation and CO_2 incorporation all occur at the cathode.

2 | Results and Discussion

2.1 | Investigations on the Reductive Generation of HAT Species

Based on the abovementioned considerations, we initiated our studies by exploring suitable HAT precursors that generate HAT species reductively at the cathode (Figure 2). Electrochemical carboxylation reactions were performed using fluorene **1** as a model substrate in the presence of 1.0 equiv. of a HAT precursor and 0.13 M of tetrabutylammonium perchlorate (NBu_4ClO_4) as an electrolyte in acetonitrile (MeCN) under a slow stream of CO_2 (1 atm) at room temperature. The reactions were conducted in a two-electrode electrochemical setup, and a constant voltage of 5.0 V was applied for 1 h using ElectraSyn 2.0 instrument (see the Supporting Information for the detailed procedure, P.S4-5) The yields shown in Figure 2 are determined by crude ^{1}H NMR analysis using 1,2-dibromoethane as the internal standard.

We first examined *p*-bromo-benzenediazonium tetrafluoroborate (**3**), *p*-methoxy-benzenediazonium tetrafluoroborate (**4**), and iodobenzene (**5**), which are known to generate aryl radicals [42] upon one-electron reduction. However, no carboxylation product was observed using **3**-**5**, indicating that simple aryl-radical-based HAT processes are ineffective under the present reductive electrochemical conditions. Next, we evaluated several carbonyl-containing HAT precursors (**6**-**10**), as these species are

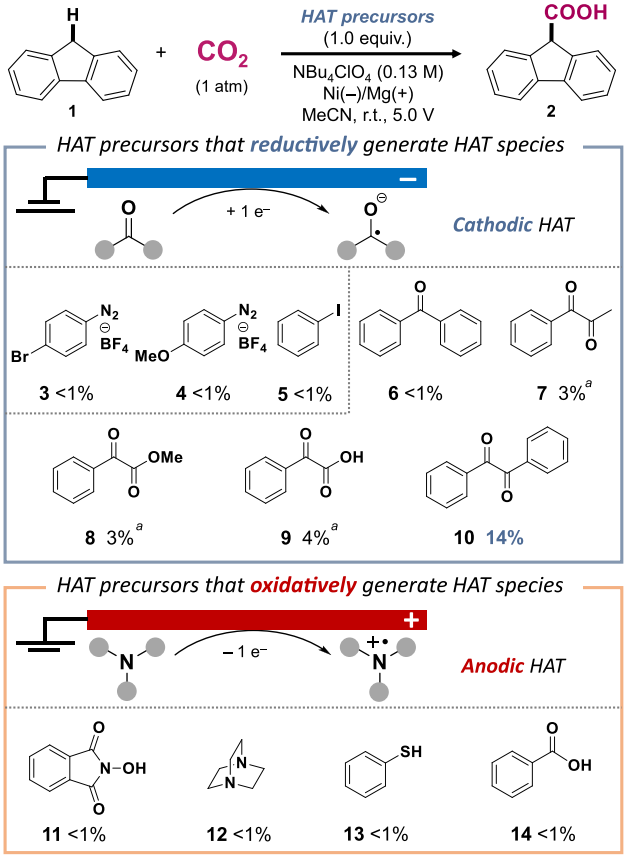

FIGURE 2 | Investigations on HAT precursors for the carboxylation of **1** with CO_2. Reaction conditions: **1** (0.50 mmol), 1 atm CO_2, HAT precursors (0.50 mmol), NBu_4ClO_4 (0.13 M) in MeCN (4.0 mL), Ni (cathode), Mg (anode), in a two-electrode electrochemical setup, 5.0 V, room temperature. Yields were determined by crude ^1H NMR analysis using 1,2-dibromoethane as the internal standard. [a]Co cathode and an applied voltage of 3.0 V were used.

known to afford ketyl radicals upon reduction [43]. Although benzophenone (**6**) did not afford the desired product, the use of 1-phenylpropane-1,2-dione (**7**) led to the formation of carboxylation product **2**, albeit in a modest yield (3%). Encouraged by this result, we further explored structurally related carbonyl compounds (**8**-**10**) and found that benzil (**10**) provided **2** in the highest yield (14%).

In contrast, commonly used HAT precursors, which oxidatively afford HAT species upon one-electron oxidation, such as *N*-hydroxyphthalimide (**11**) [44], amine (**12**) [45], thiol (**13**) [46], and carboxylic acid (**14**) [47] were entirely ineffective, and did not produce any carboxylation products under the present conditions. Because these species typically require anodic oxidation to access their active HAT species, their inactivity highlights the importance of reductive HAT generation at the cathode.

Collectively, these results indicate that carbonyl-based precursors capable of forming ketyl radicals upon cathodic reduction uniquely enable C(sp^3)–H bond carboxylation with CO_2, whereas oxidatively generated HAT precursors do not participate in the reaction. These initial studies demonstrate that the reductive generation of HAT species is essential for promoting the carboxylation reaction.

2.2 | CV

Having identified the optimal HAT precursor that reductively generates HAT species, we performed several mechanistic studies to gain insight into the reaction mechanism. We first conducted CV measurements to investigate the redox behavior of **10**. The cyclic voltammogram of **10** under an Ar atmosphere showed one reversible reduction wave at –1.53 V (*vs.* ferrocene/ferrocenium (Fc/Fc^+)) (Figure 3, blue line). We then investigated a CV measurement under a CO_2 atmosphere. Notably, the reversible reduction wave observed at –1.53 V under an Ar atmosphere became irreversible under a CO_2 atmosphere with enhanced cathodic current (Figure 3, red line). This observation suggests that the one-electron reduced species of **10** reacts with CO_2 via an electron transfer-chemical reaction (EC) process.

Furthermore, the cyclic voltammogram under CO_2 exhibited an additional reduction event at approximately –1.8 V (Figure 3, red line), indicating that the intermediate generated after the initial EC step undergoes a second one-electron reduction to produce another distinct species. (A blank CV measurement under CO_2 in the absence of **10** confirmed that this reduction event does not originate from direct CO_2 reduction (see the Supporting Information, Figure S14)). Therefore, CV analysis suggests a two-step reduction process of **10** under CO_2: (i) one-electron reduction at approximately –1.53 V (*vs.* Fc/Fc^+) followed by chemical reaction with CO_2 (EC process), (ii) further one-electron reduction to generate a second reduced species at approximately –1.8 V (*vs.* Fc/Fc^+). Interestingly, **10** was initially assumed to function solely as a precursor for cathodically generated HAT species; however, the CV measurements reveal that its reduced form displays unexpected reactivity toward CO_2.

2.3 | CV Simulations

To further examine the second reduction process described in Section 2.2, CV simulations were performed using Voltammetry simulator (For the detail, see P.S20). First, a simulation of the cyclic voltammogram of **10** under an Ar atmosphere was conducted, and the kinetic parameters were estimated (Figure 4a,b). These values were subsequently used to simulate the voltammogram under a CO_2 atmosphere.

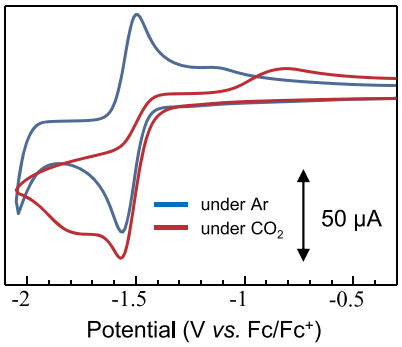

FIGURE 3 | Cyclic Voltammograms of 2.0 mM solutions of **10** under Ar (blue) and CO_2 (red) atmospheres in MeCN solutions containing 0.50 M NBu_4ClO_4. CVs were performed at a scan rate of 200 mV s^{-1} using glassy carbon (GC) as the working electrode, Ag/Ag^+ as the reference electrode, and Pt as the counter electrode.

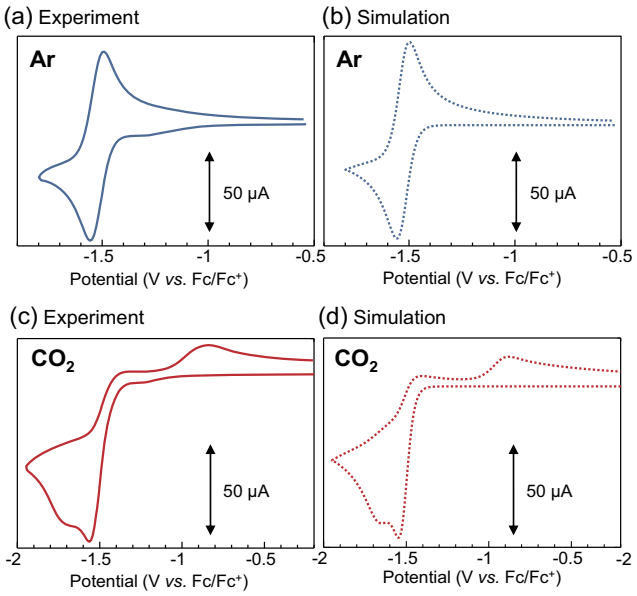

FIGURE 4 | (a) Experimental CV curves of **10** under Ar. (b) Simulation of CV curves of **10** under Ar. (c) Experimental CV curves of **10** under CO_2. (d) Simulation of CV curves of **10** under CO_2. Experimental CVs were performed in MeCN solutions containing 0.50 M NBu_4ClO_4 at a scan rate of 200 mV s^{-1} using GC as the working electrode, Ag/Ag^+ as the reference electrode, and Pt as the counter electrode.

Based on these values, a subsequent simulation was carried out for the CV under a CO_2 atmosphere (Figure 4c,d). The kinetic rate constant determined for the second electron transfer process was calculated to be on the order of 10^{-8} m/s. This value is more than two orders of magnitude lower than typical values reported for the outer-sphere electron transfer process (For the details, see P.S20) [48]. Such significant kinetic retardation strongly indicates that this reduction is not a simple electron-transfer (E) process. Instead, it is likely coupled to a concurrent chemical reaction. Combined with the experimental CV data, these results suggest that the second reduction proceeds via a chemical reaction–coupled electron-transfer pathway.

2.4 | CV and CV Simulation Under Mixed CO_2/Ar Atmospheres With Varying CO_2 Ratios

To identify the chemical reaction coupled to this second electron-transfer event, we next examined the effect of atmospheres with varying CO_2 ratios by CV. Cyclic voltammograms of **10** were measured under mixed CO_2/Ar atmospheres with CO_2 ratios of 0%, 20%, 25%, 50%, 75%, 80%, and 100% (see the Supporting Information for the detailed procedure, P.S21). As the CO_2 concentration increased, a progressive positive shift of the second reduction wave was observed, whereas the first reduction wave remained essentially unchanged (Figure 5). This observation indicates that the chemical step coupled to the second reduction involves a reaction between the one-electron-reduced species of **10** and CO_2.

To further validate this chemical step, CV simulations were performed under mixed CO_2/Ar atmospheres with varying CO_2 ratios (Figure 6a–l). The simulated voltammograms showed good

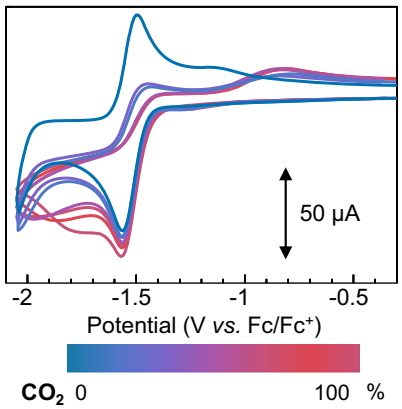

FIGURE 5 | Cyclic Voltammograms of 2.0 mM solutions of **10** under a mixed atmosphere of Ar and CO_2 in MeCN solutions containing 0.50 M NBu_4ClO_4 at a scan rate of 200 mV s^{-1} using GC as the working electrode, Ag/Ag^+ as the reference electrode, and Pt as the counter electrode. The color gradient from blue (0% CO_2, Ar atmosphere) to red (100% CO_2) reflects increasing CO_2 concentration.

agreement with the experimental data, validating the proposed reaction model. Notably, when the reduction potentials were plotted as a function of CO_2 ratio, the first reduction potential (E_1) obtained by simulation remained constant over the entire range of CO_2 ratios, while the second reduction potential (E_2) exhibited a clear dependence on CO_2 concentration (Figure 6m). This distinct difference demonstrates that the first reduction step proceeds via an EC process. On the contrary, the second reduction step is directly coupled to a chemical reaction involving CO_2 [49–52]. These results are consistent with a sequential electrochemical mechanism in which (i) an EC process at −1.53 V generates intermediate **16**, as one possible structure of the intermediate (For the detail, see the Supporting Information P.S24), followed by (ii) a CO_2-coupled electron transfer (CCET) process occurring at approximately −1.8 V to produce a further reduced species (**17**), proposed as one possible intermediate involved in the subsequent reaction steps (Figure 6n).

Collectively, these mechanistic findings demonstrate that the reduction proceeds via a CCET process, and that interaction with CO_2 is intrinsic to the formation of the subsequent reduced species. While this CCET mechanism has been proposed in several reports [49–52], their involvement in the generation of HAT species and their application to organic molecular transformations have not been reported; to the best of our knowledge, the present system represents the first example in which CCET is harnessed to generate a HAT species and enable an organic transformation. In the next section, we therefore investigate which intermediate functions as the active HAT species.

2.5 | CPE for the Carboxylation of 1 With CO_2

To determine which electrochemically generated species ((i) **16** via EC process or (ii) **17** from **16** via CCET process) functions as the active HAT species in the carboxylation reaction of **1**, CPE experiments were conducted using **1** and **10** under a CO_2 atmosphere in a three-electrode electrochemical setup equipped with

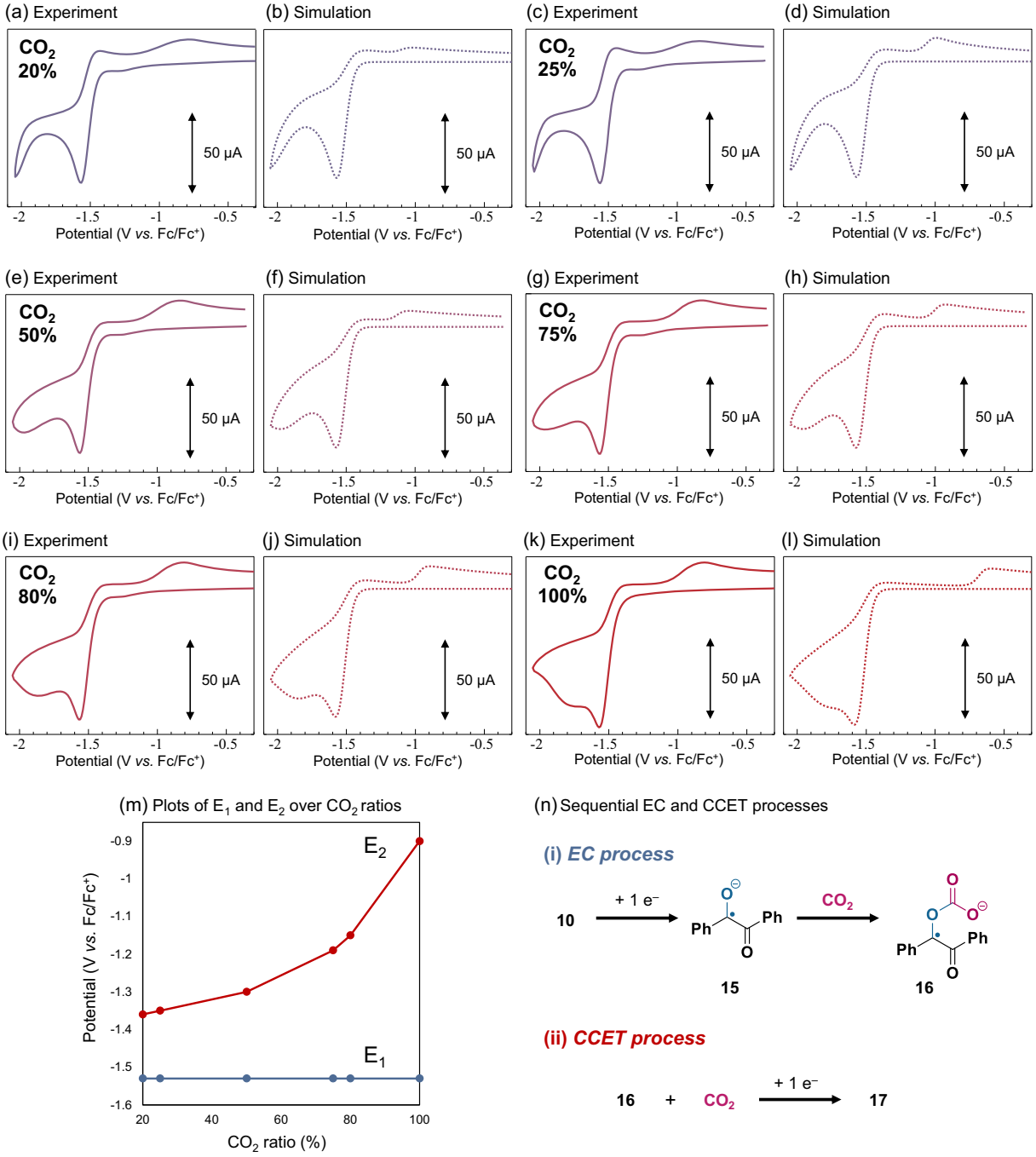

FIGURE 6 | (a) Experimental CV curves of **10** under CO_2/Ar atmospheres with a CO_2 ratio of 20%. (b) Simulation of CV curves of **10** under CO_2/Ar atmospheres with a CO_2 ratio of 20%. (c) Experimental CV curves of **10** under CO_2/Ar atmospheres with a CO_2 ratio of 25%. (d) Simulation of CV curves of **10** under CO_2/Ar atmospheres with a CO_2 ratio of 25%. (e) Experimental CV curves of **10** under CO_2/Ar atmospheres with a CO_2 ratio of 50%. (f) Simulation of CV curves of **10** under CO_2/Ar atmospheres with a CO_2 ratio of 50%. (g) Experimental CV curves of **10** under CO_2/Ar atmospheres with a CO_2 ratio of 75%. (h) Simulation of CV curves of **10** under CO_2/Ar atmospheres with a CO_2 ratio of 75%. (i) Experimental CV curves of **10** under CO_2/Ar atmospheres with a CO_2 ratio of 80%. (j) Simulation of CV curves of **10** under CO_2/Ar atmospheres with a CO_2 ratio of 80%. (k) Experimental CV curves of **10** under CO_2/Ar atmospheres with a CO_2 ratio of 100%. (l) Simulation of CV curves of **10** under CO_2/Ar atmospheres with a CO_2 ratio of 100%. (m) Plot of E_1 and E_2 obtained by the simulation over CO_2 ratios. (n) Illustration of a sequential EC and CCET processes. Experimental CVs were performed in MeCN solutions containing 0.50 M NBu_4ClO_4 at a scan rate of 200 mV s^{-1} using GC as the working electrode, Ag/Ag^+ as the reference electrode, and Pt as the counter electrode.

a reference electrode. In line with the observations by CV measurements, CPE was carried out at different applied potentials (−0.8, −1.5, −1.8, and −3.0 V *vs.* Ag/Ag^+) to selectively access the species associated with each reduction event (Figure 7a and P.S22-23). Because preparative electrolysis was conducted in a two-electrode constant-voltage mode, the cathode potential is not fixed at a single value (*vs.* Fc/Fc^+) and can vary with current, cell resistance, and overpotentials. Therefore, the CV data

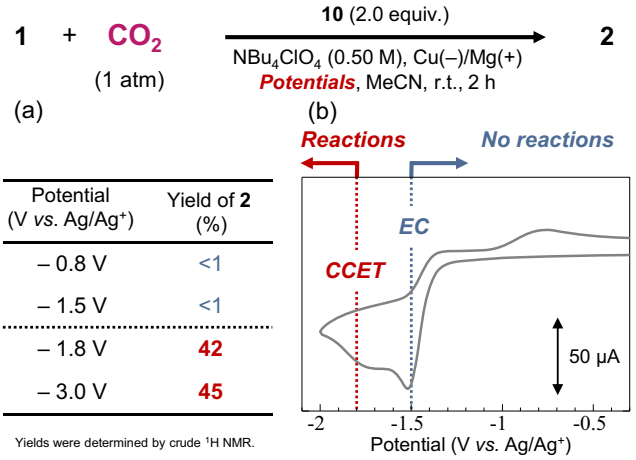

Potential (V *vs.* Ag/Ag^+)	Yield of **2** (%)
– 0.8 V	<1
– 1.5 V	<1
– 1.8 V	**42**
– 3.0 V	**45**

Yields were determined by crude ^1H NMR.

FIGURE 7 | (a) CPE of **1** under CO_2 in a three-electrode electrochemical setup at different applied potentials (–0.8, –1.5, –1.8, and –3.0 V *vs.* Ag/Ag^+). (b) Illustration of the relationship between the applied potentials and the reaction outcome in CV curves of **1** under CO_2.

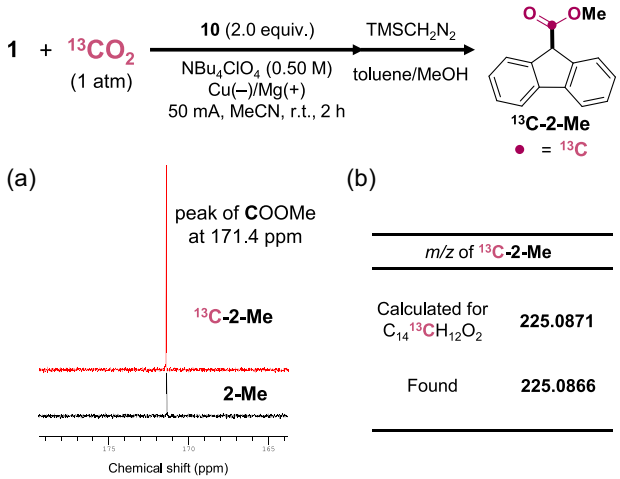

m/z of ^{13}C-**2-Me**	
Calculated for $C_{14}{}^{13}CH_{12}O_2$	**225.0871**
Found	**225.0866**

FIGURE 8 | (a) ^{13}C NMR spectra showing the signal of the carboxyl carbon (171.4 ppm) for the isolated products (**^{13}C-2-Me** and **2-Me**) from the ^{13}C isotope labeling experiment (red line) and the standard conditions (black line). (b) HRMS analysis of the product (**^{13}C-2-Me)** from the isotope labeling experiment.

are used here to identify feasible reduction events and to rationalize the sequence of redox/chemical steps, rather than to define the exact operating potential during electrolysis.

CPE at –0.8 and –1.5 V did not produce any carboxylation product **2**, indicating that the species formed exclusively through the initial EC process ((i), at approximately –1.53 V in the CV study), did not participate in the carboxylation reaction. In sharp contrast, electrolysis at –1.8 V afforded **2** in 42% yield, and a comparable reactivity (45%) was observed at –3.0 V.

These results indicate that only the species formed after the CCET event (**17**, in Figure 6n) is responsible for enabling the carboxylation reaction (Figure 7b). On the contrary, the species generated solely through the EC process does not exhibit any reactivity toward the reaction. Collectively, these CPE experiments suggest that the cathodically generated species formed after the sequential EC-CCET processes function as the active HAT species responsible for promoting the carboxylation reaction. Moreover, although a deprotonation pathway involving the radical anion **15** could be considered based on the acidity, these CPE experiments suggest that such a pathway is unlikely under the present reaction conditions.

2.6 | Isotope Labeling Experiment

A ^{13}C Isotope labeling experiment was conducted to verify the source of the carboxyl moiety in product **2**. Owing to the difficulty in isolating the ^{13}C-labeled carboxylic acid, the product was converted into the corresponding methyl ester **^{13}C-2-Me** prior to analysis. Accordingly, the carboxylation reaction was performed using $^{13}CO_2$, and the desired product, **^{13}C-2-Me**, was obtained as the methyl ester form. The ^{13}C NMR analysis of **^{13}C-2-Me** exhibited a prominent signal at 171.4 ppm, which reveals the ^{13}C incorporation at the carboxyl group (Figure 8a and the Supporting Information P.S25-27). Moreover, high-resolution mass spectrometry (HRMS) confirmed ^{13}C-contained product **^{13}C-2-Me** (Figure 8b, m/z $[M]^+$calcd for $C_{14}{}^{13}CH_{12}O_2$ 225.0871; Found 225.0866, also see P.S28).

Therefore, these results clearly confirm that the carboxyl group of the product is derived from CO_2 gas.

2.7 | Proposed Reaction Mechanism

Based on these mechanistic investigations, a plausible reaction mechanism is proposed for our system (Figure 9). The reaction is initiated by cathodic reduction of **10**, followed by the reaction with CO_2 via (i) an EC process, as supported by CV measurements. The resulting intermediate is proposed to be carbonate intermediate **16** [53], as suggested by ^{13}C NMR analysis after CPE of **10** under CO_2 (see the Supporting Information, P.S24). Subsequent one-electron reduction via (ii) a CCET process may generate the active HAT species **17**, proposed as one possible candidate responsible for the subsequent $C(sp^3)$—H bond activation, consistent with the results of CV simulations and CPE experiments .

The thus-formed active HAT species, represented as **17**, may abstract a hydrogen atom from the benzylic $C(sp^3)$—H bond

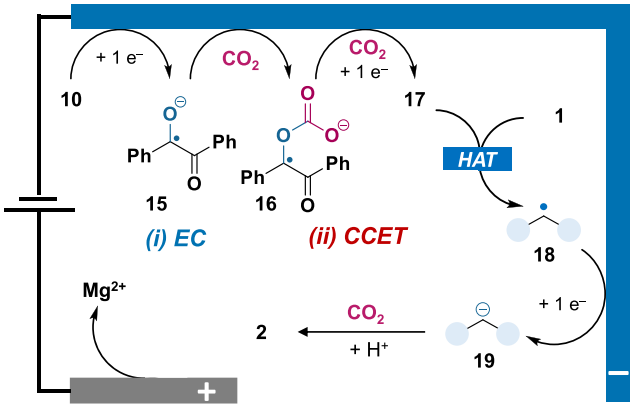

FIGURE 9 | Plausible reaction mechanism.

of **1**, yielding the radical **18** (the evaluation of BDE values of C(sp^3)—H bonds in **1** and possible intermediates determined by density functional theory (DFT) calculations, see P.S29-30). This radical is further reduced at the cathode, giving the anion intermediate **19**. Finally, the nucleophilic addition of **19** to CO_2 and, upon protonation, produces the desired carboxylation product **2**. Meanwhile, at the anode, the sacrificial electrode (Mg) would supply the electron to the system for sustaining the electrochemical process.

Notably, these mechanistic findings demonstrate that the reductive generation of HAT species at the cathode is crucial for achieving efficient carboxylation of C(sp^3)—H bonds with CO_2 under mild conditions, and represent a fundamental mechanistic distinction from previously reported strategies.

2.8 | Optimization Studies

Having established that cathodically generated HAT species formed via (i) EC and (ii) CCET pathways are responsible for productive C(sp^3)—H bond carboxylation, we next turned our attention to optimizing the electrochemical reaction conditions to improve the overall efficiency (Table 1). We first evaluated the influence of electrode materials. Product yield was strongly dependent on the cathode/anode electrode combination. The replacement of the Mg anode with Zn (entry 2) or Al (entry 3) resulted in significantly lower yields. Screening of the cathode electrodes (entries 4–7) revealed the Co(−)/Mg(+) couple of electrodes as the optimum electrodes (entry 7). At this stage, the incomplete recovery of starting material **1** remained problematic. To improve substrate recovery and reduce energy consumption, the applied voltage was lowered from 5.0 V to 3.0 V for further studies (entries 8–12).

Although the yield of **2** decreased initially (12%, entry 8), extending the reaction time from 1 to 3 h (22%, entry 9) and increasing the amount of **10** to 2 equivalents resulted in a modest improvement (entry 10, up to 30%). Notably, the use of a more concentrated NBu_4ClO_4 electrolyte (0.50 M) significantly enhanced the yield to 61% (entry 11). Under the optimized conditions, in the presence of 2 equiv. of **10**, 0.50 M NBu_4ClO_4 in MeCN with Co(−)/Mg(+) couple of the electrodes under an applied voltage of 3.0 V for 2 h, **2** was produced in 69% yield. Control experiments confirmed that the reaction did not proceed in the absence of either **10** (entry 13), CO_2 (entry 14), or the electrolysis (entry 15), suggesting that they are all indispensable to the reaction. Additional experiments showed that substoichiometric or catalytic amounts of benzil resulted in significantly decreased yields (P.S15). Furthermore, the details of Faradaic efficiency measurements, electrolyte and electrode effects, preliminary substrate scope studies, and the isolated yield are provided in the Supporting Information (P.S13–17).

Overall, these optimization studies demonstrate that efficient electrochemical carboxylation of C(sp^3)—H bonds is achieved by integrating mechanistic insights into cathodically generated HAT activation with the appropriate selection of electrochemical parameters.

TABLE 1 | Optimization studies on the electrochemical reaction conditions.

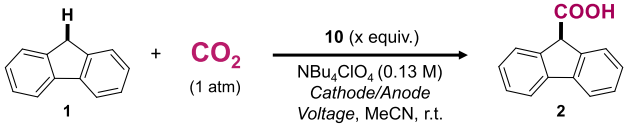

Entry	Cathode	Anode	Voltage	*x*	Time	Yield (%)[b]
1	Ni	Mg	5	1	1	14
2	Ni	Zn	5	1	1	2
3	Ni	Al	5	1	1	<1
4	GC	Mg	5	1	1	9
5	Mg	Mg	5	1	1	<1
6	Cu	Mg	5	1	1	23
7	Co	Mg	5	1	1	26
8	Co	Mg	3	1	1	12
9	Co	Mg	3	1	3	22
10	Co	Mg	3	2	3	30
11[c]	Co	Mg	3	2	3	61
12[c]	Co	Mg	3	2	2	69

Entry	Deviation from entry 12	Yield (%)[b]
13	Without **10**	< 1
14	Under Ar atmosphere	< 1
15	Without electrolysis	< 1

[a]Reaction conditions: **1** (0.50 mmol), 1 atm CO_2, **10**, NBu_4ClO_4 (0.13 M) in MeCN (4.0 mL), room temperature.
[b]Yields were determined by crude ^1H NMR analysis using 1,2-dibromoethane or 1,1,2,2-tetrachloroethane as the internal standard.
[c]0.50 M of NBu_4ClO_4 was used.

3 | Conclusion

In conclusion, we have developed a new electrochemical system for the carboxylation of dibenzylic C(sp^3)—H bonds with CO_2. The reaction proceeds efficiently under mild conditions, affording the corresponding carboxylation product in good yield (up to 69%) at room temperature under a 1 atm CO_2 atmosphere. The key to this achievement is the use of the HAT species reductively generated at the cathode to activate C(sp^3)—H bonds, representing a rare example of C(sp^3)—H bond functionalization mediated by cathodically-generated HAT species. Notably, in contrast to the pioneering report by Qiu et al., which requires diffusion of the reaction intermediate between the electrodes, our system enables all key elementary steps (generation of HAT species, C(sp^3)—H bond cleavage, and CO_2 incorporation) to occur at the same cathode electrode. Moreover, mechanistic studies support a plausible reaction mechanism involving sequential EC and CCET processes for the generation of the active HAT species. Notably, our initial working hypothesis assumed that the cathodically reduced HAT precursor would directly abstract a hydrogen atom from the substrate. However, detailed electrochemical and spectroscopic analyses revealed an unexpected mechanistic feature: the reduced species preferentially reacts with CO_2, and the resulting CO_2-derived intermediate subsequently serves as the active HAT species responsible for C(sp^3)—H bond activation. This finding highlights that CO_2 is not merely a coupling partner incorporated after C(sp^3)—H bond activation, but rather plays an intrinsic role in the generation of the reactive HAT species itself. On the basis of this mechanistic insight, the present system can be regarded as a cathodic reaction platform in which CO_2 capture and reductive HAT generation are intrinsically coupled. In other words, the key reaction components, electrons, HAT species, and CO_2, are compactly integrated at a single cathodic interface. This integrated reaction environment provides a mechanistic framework for understanding the observed reactivity and is expected to enable further improvements in reaction yield, rate, and generality in future developments. Collectively, this study establishes a fundamentally distinct and practical strategy for C(sp^3)—H bond functionalization based on reductively generated HAT species, opening new avenues for electrochemical transformations of inert chemical bonds.

Acknowledgments

This work was supported by the Japan Society for the Promotion of Science KAKENHI [Grant Nos. 22K21348, 23H04903 (Green Catalysis Science), and 24H00464 (S.M.); 22K06525 and 25K22528 (Y.S.); 23K26766 (M.H.); 22H04507, 23H02043, and 25H01671 (T.K.); 22K19086, 23H04628, 24H02212 (Chemical Structure Reprogramming (SReP)), and 25H00885 (M.K.)], Japan Science and Technology Agency (JST) CREST [Grant No. JPMJCR20B6 (S.M.)] and JST FOREST [Grant No. JPMJFR223I (T.K.) and Grant Nos. JPMJFR221S (M.K.)]. Funding was received from the Fujimori Science and Technology Foundation (Y.S.), Kato Foundation for Promotion of Science (KJ-3413) (T.K.), ENEOS Hydrogen Trust Fund (M.K.), and the Mitsubishi Foundation (M.K.). The authors thank Dr. Hiroaki Tanaka (Analytical Instrumentation Facility, the University of Osaka) for HRMS measurements. The authors also thank the Analytical Instrumentation Facility of the University of Osaka for access to the instrumentation used in this work. This work used the research equipment shared in the MEXT Project for promoting public utilization of advanced research infrastructure (Program for Supporting Construction of Core Facilities) Grant Number [JPMXS0441200025].

Funding

This study was supported by Japan Society for the Promotion of Science (22K21348, 23H04903, 24H00464, 22K06525, 25K22528, 23K26766, 22H04507, 23H02043, 25H01671, 22K19086, 23H04628, 24H02212, 25H00885); Core Research for Evolutional Science and Technology (JPMJCR20B6); Fusion Oriented Research for disruptive Science and Technology (JPMJFR223I, JPMJFR221S); Fujimori Science and Technology Foundation; Kato Foundation for Promotion of Science (KJ-3413); ENEOS Hydrogen Trust Fund; Mitsubishi Foundation.

Conflicts of Interest

The authors declare no conflicts of interest.

Data Availability Statement

The data that support the findings of this study are available from the corresponding author upon reasonable request.

References

1. M. He, Y. Sun, and B. Han, "Green Carbon Science: Scientific Basis for Integrating Carbon Resource Processing, Utilization, and Recycling," *Angewandte Chemie International Edition* 52 (2013): 9620–9633.

2. M. Aresta, A. Dibenedetto, and A. Angelini, "Catalysis for the Valorization of Exhaust Carbon: From CO_2 to Chemicals, Materials, and Fuels. Technological Use of CO_2," *Chemical Reviews* 114 (2014): 1709–1742.

3. Q.-W. Song, Z.-H. Zhou, and L.-N. He, "Efficient, Selective and Sustainable Catalysis of Carbon Dioxide," *Green Chemistry* 19 (2017): 3707–3728.

4. B. Grignard, S. Gennen, C. Jérôme, A. W. Kleij, and C. Detrembleur, "Advances in the Use of CO_2 as a Renewable Feedstock for the Synthesis of Polymers," *Chemical Society Reviews* 48 (2019): 4466–4514.

5. K. Huang, C.-L. Sun, and Z.-J. Shi, "Transition-Metal-Catalyzed C–C Bond Formation through the Fixation of Carbon Dioxide," *Chemical Society Reviews* 40 (2011): 2435–2452.

6. Q. Liu, L. Wu, R. Jackstell, and M. Beller, "Using Carbon Dioxide as a Building Block in Organic Synthesis," *Nature Communications* 6 (2015): 5933.

7. A. Tortajada, F. Juliá-Hernández, M. Börjesson, T. Moragas, and R. Martin, "Transition-Metal-Catalyzed Carboxylation Reactions with Carbon Dioxide," *Angewandte Chemie International Edition* 57 (2018): 15948–15982.

8. J.-H. Ye, T. Ju, H. Huang, L.-L. Liao, and D.-G. Yu, "Radical Carboxylative Cyclizations and Carboxylations with CO_2," *Accounts of Chemical Research* 54 (2021): 2518–2531.

9. S. Pimparkar, A. K. Dalvi, A. Koodan, et al., "Recent Advances in the Incorporation of CO_2 for C–H and C–C Bond Functionalization," *Green Chemistry* 23 (2021): 9283–9317.

10. R. Cauwenbergh, V. Goyal, R. Maiti, K. Natte, and S. Das, "Challenges and Recent Advancements in the Transformation of CO_2 into Carboxylic Acids: Straightforward Assembly with Homogeneous 3d Metals," *Chemical Society Reviews* 51 (2022): 9371–9423.

11. G.-Q. Sun, L.-L. Liao, C.-K. Ran, J.-H. Ye, and D.-G. Yu, "Recent Advances in Electrochemical Carboxylation with CO_2," *Accounts of Chemical Research* 57 (2024): 2728–2745.

12. H. Maag, *Prodrugs of Carboxylic Acids* (Springer, 2007).

13. S. Pradhan and S. Das, "Recent Advances on the Carboxylations of C(sp^3)–H Bonds Using CO_2 as the Carbon Source," *Synlett* 34 (2023): 1327–1342.

14. T. G. Saint-Denis, R.-Y. Zhu, G. Chen, Q.-F. Wu, and J.-Q. Yu, "Enantioselective C(sp^3)–H Bond Activation by Chiral Transition Metal Catalysts," *Science* 359 (2018): 759.

15. J. C. K. Chu and T. Rovis, "Complementary Strategies for Directed C(sp^3)-H Functionalization: A Comparison of Transition-Metal-Catalyzed Activation, Hydrogen Atom Transfer, and Carbene/Nitrene Transfer," *Angewandte Chemie International Edition* 57 (2018): 62–101.

16. R. R. Karimov and J. F. Hartwig, "Transition-Metal-Catalyzed Selective Functionalization of C(sp^3)-H Bonds in Natural Products," *Angewandte Chemie International Edition* 57 (2018): 4234–4241.

17. B. Liu, A. M. Romine, C. Z. Rubel, K. M. Engle, and B.-F. Shi, "Transition-Metal-Catalyzed, Coordination-Assisted Functionalization of Nonactivated C(sp^3)–H Bonds," *Chemical Reviews* 121 (2021): 14957–15074.

18. J. Grover, A. T. Sebastian, S. Maiti, A. C. Bissember, and D. Maiti, "Unified Approaches in Transition Metal Catalyzed C(sp^3)–H Functionalization: Recent Advances and Mechanistic Aspects," *Chemical Society Reviews* 54 (2025): 2006–2053.

19. K. Michigami, T. Mita, and Y. Sato, "Cobalt-Catalyzed Allylic C(sp^3)-H Carboxylation with CO_2," *Journal of the American Chemical Society* 139 (2017): 6094–6097.

20. M. Shigeno, K. Sasaki, K. Nozawa-Kumada, and Y. Kondo, "Double-Carboxylation of Two C−H Bonds in 2-Alkylheteroarenes Using LiO-tBu/CsF," *Organic Letters* 21 (2019): 4515–4519.

21. M. Shigeno, I. Tohara, K. Sasaki, K. Nozawa-Kumada, and Y. Kondo, "Combined Brønsted Base-Promoted CO_2 Fixation into Benzylic C-H Bonds of Alkylarenes," *Organic Letters* 24 (2022): 4825–4830.

22. Y. Masuda, N. Ishida, and M. Murakami, "Light-Driven Carboxylation of oAlkylphenyl Ketones with CO_2," *Journal of the American Chemical Society* 137 (2015): 14063–14066.

23. N. Ishida, Y. Masuda, S. Uemoto, and M. Murakami, "A Light/Ketone/Copper System for Carboxylation of Allylic C–H Bonds of Alkenes with CO_2," *Chemistry-A European Journal* 22 (2016): 6524–6527.

24. H. Seo, M. H. Katcher, and T. F. Jamison, "Photoredox Activation of Carbon Dioxide for Amino Acid Synthesis in Continuous Flow," *Nature Chemistry* 9 (2017): 453–456.

25. Y.-Y. Gui, W.-J. Zhou, J.-H. Ye, and D.-G. Yu, "Photochemical Carboxylation of Activated C(sp^3)–H Bonds with CO_2," *ChemSusChem* 10 (2017): 1337–1340.

26. Q.-Y. Meng, T. E. Schirmer, A. L. Berger, K. Donabauer, and B. König, "Photocarboxylation of Benzylic C−H Bonds," *Journal of the American Chemical Society* 141 (2019): 11393–11397.

27. N. Ishida, Y. Masuda, Y. Imamura, K. Yamazaki, and M. Murakami, "Carboxylation of Benzylic and Aliphatic C-H Bonds with CO_2 Induced by Light/Ketone/Nickel," *Journal of the American Chemical Society* 141 (2019): 19611–19615.

28. Y. Liu, G.-H. Xue, Z. He, et al., "Visible-Light Photoredox-Catalyzed Direct Carboxylation of Tertiary C(sp^3)–H Bonds with CO_2: Facile Synthesis of All-Carbon Quaternary Carboxylic Acids," *Journal of the American Chemical Society* 146 (2024): 28350–28359.

29. J.-L. Li, S.-S. Zhang, L.-L. Jiang, et al., "Redox-Neutral Carboxylation of Benzylic Tertiary C-H Bonds with Carbon Dioxide," *Angewandte Chemie International Edition* 64 (2025): e202420852.

30. M. Yan, Y. Kawamata, and P. S. Baran, "Synthetic Organic Electrochemical Methods Since 2000: On the Verge of a Renaissance," *Chemical Reviews* 117 (2017): 13230–13319.

31. C. Kingston, M. D. Palkowitz, Y. Takahira, et al., "A Survival Guide for the Electro-Curious," *Accounts of Chemical Research* 53 (2020): 72–83.

32. J. C. Siu, N. Fu, and S. Lin, "Catalyzing Electrosynthesis: A Homogeneous Electrocatalytic Approach to Reaction Discovery," *Accounts of Chemical Research* 53 (2020): 547–560.

33. N. E. S. Tay, D. Lehnherr, and T. Rovis, "Photons or Electrons? A Critical Comparison of Electrochemistry and Photoredox Catalysis for Organic Synthesis," *Chemical Reviews* 122 (2022): 2487–2649.

34. J. Rein, S. B. Zacate, K. Mao, and S. Lin, "A Tutorial on Asymmetric Electrocatalysis," *Chemical Society Reviews* 52 (2023): 8106–8125.

35. W. Zeng, C. Peng, and Y. Qiu, "Electrochemical Benzylic C-H Carboxylation," *Journal of the American Chemical Society* 147 (2025): 13461–13470.

36. L. Capaldo, D. Ravelli, and M. Fagnoni, "Direct Photocatalyzed Hydrogen Atom Transfer (HAT) for Aliphatic C−H Bonds Elaboration," *Chemical Reviews* 122 (2022): 1875–1924.

37. Y. Liang, X. Zhan, F. Li, et al., "Using a Nitrogen-Centered Radical as a Selective Mediator in Electrochemical C(sp^3)-H Amination," *Chem Catalysis* 3 (2023): 100582.

38. Y. Morii, T. Watanabe, Y. Saga, T. Kambe, M. Kondo, and S. Masaoka, "Electrochemical C(sp^3)−H Functionalization Using Acetic Acid as a Hydrogen Atom Transfer Reagent," *ChemElectroChem* 11 (2024): e202400061.

39. K. Mukherjee, A. B. David, H. Nikoghosyan, R. Hakobyan, and V. Gevorgyan, "Light-Induced Transition-Metal-Catalysed Hydrogen Atom Transfer in Organic Transformations," *Nature Catalysis* 8 (2025): 1146–1158.

40. L. Rapisarda, A. Fermi, P. Ceroni, R. Giovanelli, G. Bertuzzi, and M. Bandini, "Electrochemical C(sp^3)–H Functionalization of Ethers via Hydrogen-Atom Transfer by Means of Cathodic Reduction," *Chemical Communication* 59 (2023): 2664–2667.

41. S. Zhang and M. Findlater, "Electrochemically Driven Hydrogen Atom Transfer Catalysis: A Tool for C(sp^3)/Si–H Functionalization and Hydrofunctionalization of Alkenes," *ACS Catalysis* 13 (2023): 8731–8751.

42. Z. Wu, K. Li, M. Liao, et al., "Photoinduced Copper-Catalyzed Enantioselective Alkylalkynylation of Alkenes via Polarity-Matched Hydrogen Atom Transfer," *Journal of the American Chemical Society* 147 (2025): 22072–22083.

43. J. A. Dantas, J. T. M. Correia, M. W. Paixão, and A. G. Corrêa, "Photochemistry of Carbonyl Compounds: Application in Metal–Free Reactions," *ChemPhotoChem* 3 (2019): 506–520.

44. J. Ke, W. Liu, X. Zhu, X. Tan, and C. He, "Electrochemical Radical Silyl-Oxygenation of Activated Alkenes," *Angewandte Chemie International Edition* 60 (2021): 8744–8749.

45. M. H. Shaw, V. W. Shurtleff, J. A. Terrett, J. D. Cuthbertson, and D. W. C. MacMillan, "Native Functionality in Triple Catalytic Cross-Coupling: Sp^3 C–H Bonds as Latent Nucleophiles," *Science* 352 (2016): 1304–1308.

46. K. Qvortrup, D. A. Rankic, and D. W. C. MacMillan, "A General Strategy for Organocatalytic Activation of C−H Bonds via Photoredox Catalysis: Direct Arylation of Benzylic Ethers," *Journal of the American Chemical Society* 136 (2014): 626–629.

47. S. Mukherjee, B. Maji, A. Tlahuext-Aca, and F. Glorius, "Visible-Light-Promoted Activation of Unactivated C(sp^3)−H Bonds and Their Selective Trifluoromethylthiolation," *Journal of the American Chemical Society* 138 (2016): 16200–16203.

48. R. Kaur, A. Ghoshal, P. Galav, and P. C. Mondal, "Electrochemical Charge Transfer Kinetics of Ferrocene in the Light of Different Working Electrodes," *Chemistry An Asian Journal* 19 (2024): e202400744.

49. Y. Liu, H.-Z. Ye, K. M. Diederichsen, T. V. Voorhis, and T. A. Hatton, "Electrochemically Mediated Carbon Dioxide Separation with Quinone Chemistry in Salt-Concentrated Aqueous Media," *Nature Communications* 11 (2020): 2278.

50. A. T. Bui, N. A. Hartley, A. J. W. Thom, and A. C. Forse, "Trade-Off between Redox Potential and the Strength of Electrochemical CO_2 Capture in Quinones," *The Journal of Physical Chemistry C* 126 (2022): 14163–14172.

51. A. M. Zito, D. Bím, S. Vargas, A. N. Alexandrova, and J. Y. Yang, "Computational and Experimental Design of Quinones for Electrochemical CO_2 Capture and Concentration," *ACS Sustainable Chemistry & Engineering* 10 (2022): 11387–11395.

52. M. Abdinejad, M. Massen-Hane, H. Seo, and T. A. Hatton, "Oxygen-Stable Electrochemical CO_2 Capture Using Redox-Active Heterocyclic Benzodithiophene Quinone," *Angewandte Chemie International Edition* 63 (2024): e202412229.

53. X. Li, X. Zhao, L. Zhang, et al., "Redox-Tunable Isoindigos for Electrochemically Mediated Carbon Capture," *Nature Communications* 15 (2024): 1175.

54. S. Bazzi, E. Schultz, and M. Mellah, "Electrogenerated Sm(II)-Catalyzed CO_2 Activation for Carboxylation of Benzyl Halides," *Organic Letters* 21 (2019): 10033–10037.

55. J. Kim, Y. Ohk, S. H. Park, Y. Jung, and S. Chang, "Intramolecular Aromatic Carbenoid Insertion of Biaryldiazoacetates for the Regioselective Synthesis of Fluorenes," *Chemistry – An Asian Journal* 6 (2011): 2040–2047.

56. C. Guo, Y. Zhang, and Y. Zhang, "An Efficient Approach for Enhancing the Catalytic Activity of Ni-MOF-74 *via* a Relay Catalyst System for the Selective Oxidation of Benzylic C–H Bonds under Mild Conditions," *Chemical Communications* 54 (2018): 3701–3704.

57. A. D. Becke, "Density-Functional Thermochemistry. III. The Role of Exact Exchange," *The Journal of Chemical Physics* 98 (1993): 5648–5652.

58. C. Lee, W. Yang, and R. G. Parr, "Development of the Colle-Salvetti Correlation-Energy Formula into a Functional of the Electron Density," *Physical Review B* 37 (1988): 785.

59. J. Tomasi, B. Mennucci, and R. Cammi, "Quantum Mechanical Continuum Solvation Models," *Chemical Reviews* 105 (2005): 2999–3094.

60. H. Nakai and A. Ishikawa, "Quantum Chemical Approach for Condensed-Phase Thermochemistry: Proposal of a Harmonic Solvation Model," *The Journal of Chemical Physics* 141 (2014): 174106.

61. M. J. Frisch, G. W. Trucks, H. B. Schlegel, et al., *Gaussian 16, Revision C.01* (Gaussian, Inc., 2016).

Supporting Information

Additional supporting information can be found online in the Supporting Information section. The authors have cited additional references within the Supporting Information [54–61].